SHAPE OPTIMIZATION OF SHAFTS FOR DESIRED EIGENFREQUENCIES IN ROTATING SYSTEMS

Rodrigo Nicoletti, rnicolet@sc.usp.br
Universidade de São Paulo
Escola de Engenharia de São Carlos
Departamento de Engenharia Mecânica
Av. trabalhador São-Carlense, 400
13566-590 São Carlos - SP, Brasil

Abstract. *Rotating machines are commonly analyzed by mathematical models based on finite shaft elements. This procedure is straightforward and enables the engineer to calculate critical speeds, mode shapes, and frequency response functions of the system by setting the geometric properties of the shaft. On the other hand, the inverse problem of finding the geometry of the shaft as a function of desired parameters, such as critical speeds and eigenfrequencies, is not as thoroughly investigated as the direct problem. In this work, one presents a procedure for finding the shaft geometry as a function of desired eigenfrequencies of the system, based on sensitivity functions and matrix properties of the finite shaft element. By setting the desired eigenvalues of the rotating system, the objective functions are minimized by a Newton-Raphson algorithm, whose Jacobian matrix is composed of the eigenvalue sensitivity functions. The chosen design variables are the radii of shaft elements. The eigenvalue sensitivity functions are obtained by taking advantage of the fact that finite element matrices are functions of the shaft radius. As a result, one achieves a practical, low time consuming, procedure for checking and adjusting the shaft geometry as a function of the desired eigenfrequencies and critical speeds of rotating machines, in early stages of design.*

Keywords: *shape optimization, parameter sensitivity, rotor dynamics, rotor modeling, eigenanalysis*

1. INTRODUCTION

Rotating machines are designed for specific operational conditions and, the dynamic characteristics of such machines must fulfill the requirements defined by these operational conditions. This means that, the engineer must have knowledge of critical speeds, frequency response functions and overall vibration levels that the machine in design will present under operation. This information must not conflict with the previously defined design requirements.

Several parameters have influence on the final dynamic characteristics of rotating machines. Among these parameters, one can list the bearing equivalent damping and stiffness and, the rotor geometry. By defining these parameters in the design process, the engineer basically sets the final dynamic characteristics of the rotating machine. Hence, it is important to the engineer to gain some insight into the sensitivity of the system dynamics to these parameters, in order to choose the appropriated values for each one. This kind of information can help the engineer to identify critical parameters and choose the optimum, or near optimum, design solution, resulting in a machine that presents dynamic characteristics that fulfill the design requirements. The optimum design solution can be obtained by many different ways and, in many cases, it is not a trivial task.

The sensitivity analysis of rotating machines can be based on empirical experience or on correlated mathematical models. The first case is viable when there is much information on a machine that already exists, and the machine is being redesigned with minor changes. If this is not the case, the engineer must rely on the second alternative: models. Many works can be found in literature related to sensitivity analyses on rotating machines based on rotor dynamic models. In most of the cases, the design parameters in study are the bearing characteristics. For instance, Huang and Lin (2002) present a sensitivity analysis of the critical speeds of a rotor modeled by finite elements. By minimizing a functional, the authors find the optimum values of support stiffness that locate the critical speeds of the system in desired frequencies. Fang and Wang (2003) optimize the parameters of hydrodynamic bearings to minimize rotor support forces and, consequently, response functions. The sensitivity analysis also helped finding the appropriated positions to locate the bearings. Silveira and Lucchesi (2004) adopted a Design of Experiments Method to perform the sensitivity analysis of the system to bearing parameters. In their work, the vibration levels of the rotor under first bending frequency were minimized, numerically and experimentally.

One of the first works related to the sensitivity analysis of rotating systems to geometric properties is presented by Lund (1980). In his work, the author estimates the percentage of change in final critical speeds by the percentage of change in the geometric properties of the rotor, through a state vector transfer matrix. By this methodology, the critical elements in the rotor can be identified and properly changed to desired results. In the same direction, Rajan et al. (1986) perform sensitivity analyses on a rotor modeled by finite elements, where the design parameters are the length and inertia properties of the elements. The authors take advantage of properties of the element matrices that simplify the analysis, and whose results allow the identification of the critical elements to vibration levels and mode shapes. Acceptable results were obtained by changing up to 20% the original values of the system.

In this work, one presents a procedure for finding the shaft geometry as a function of desired eigenfrequencies of the system, based on sensitivity functions and matrix properties of the finite shaft element. By setting the desired eigenvalues of the rotating system, the objective functions are minimized by a Newton-Raphson algorithm, whose Jacobian matrix is composed of the eigenvalue sensitivity functions. The chosen design variables are the radii of shaft elements. The eigenvalue sensitivity functions are obtained by taking advantage of the fact that finite element matrices are functions of the shaft radius. As a result, one achieves a practical, low time consuming, procedure for checking and adjusting the shaft geometry as a function of the desired eigenfrequencies and critical speeds of rotating machines, in early stages of design. The procedure can also be used for model updating, setting the experimentally measured frequencies as desired frequencies, and obtaining the updated shaft shape (radii) to be used in the model.

2. FINITE ELEMENT FORMULATION OF ROTATING SYSTEMS

Nelson and McVaugh (1976) proposed a methodology for modeling rotors using finite elements and, since then, this methodology has been widely used and incorporated into simulation commercial softwares. The idea is to divide the shaft in several segments (elements) whose geometry can be represented by a cylinder of constant radius. The authors based the formulation of the shaft finite elements on Euler-Bernoulli beam assumptions, thus being suitable for slender shafts whose shear stresses in bending can be neglected ($L/D > 10$).

Each shaft element has a translational mass matrix ($\mathbf{M}_e^T$), a rotational mass matrix ($\mathbf{M}_e^R$), a gyroscopic matrix ($\mathbf{G}_e$), and a stiffness matrix ($\mathbf{K}_e$), resulting to the following equation of motion for one shaft element:

$$\left(\mathbf{M}_e^T + \mathbf{M}_e^R\right)\ddot{\mathbf{q}}_e - \Omega\,\mathbf{G}_e\,\dot{\mathbf{q}}_e + \mathbf{K}_e\,\mathbf{q}_e = \mathbf{0} \tag{1}$$

where $\mathbf{q}_e$ is the nodal displacement vector, containing the eight degrees-of-freedom of the shaft element (two translations and two rotations in each node).

By combining the individual matrices of each shaft element, one can obtain the global matrices that represent the whole shaft, thus resulting to the following equation of motion:

$$\left(\mathbf{M}^T + \mathbf{M}^R\right)\ddot{\mathbf{q}} - \Omega\,\mathbf{G}\,\dot{\mathbf{q}} + \mathbf{K}\,\mathbf{q} = \mathbf{0} \tag{2}$$

where $\mathbf{M}^T$ is the global translational mass matrix, $\mathbf{M}^R$ is the global rotational mass matrix, $\mathbf{G}$ is the global gyroscopic matrix, $\mathbf{K}$ is the global stiffness matrix, and $\mathbf{q}$ is the displacement vector containing all $4(n_e+1)$ degrees-of-freedom of the shaft elements that represent the physical shaft (n_e is the number of shaft elements).

The simplicity of the method lies on the fact that bearings and disks (a simplified model for a pump or a turbine) can also be represented by matrices: the bearings are represented by stiffness and damping matrices and, the disks are represented by inertia and gyroscopic matrices. Hence, one can include bearing and disks in the model by adding their respective matrices to the global matrices of the shaft, in the positions relative to the degrees-of-freedom of the nodes they are attached to. By including the bearing and disks models, one arrive at the global equation of motion of the rotating system:

$$\mathbf{M}\,\ddot{\mathbf{q}} + (\mathbf{D} - \Omega\,\mathbf{G})\,\dot{\mathbf{q}} + \mathbf{K}\,\mathbf{q} = \mathbf{0} \tag{3}$$

where $\mathbf{M}$ is the global inertia matrix including shaft translational and rotational inertia and disk inertia effects, $\mathbf{D}$ is the global damping matrix including bearing damping effects, $\mathbf{G}$ is the global gyroscopic matrix including shaft and disk gyroscopic effects and, $\mathbf{K}$ is the global stiffness matrix including shaft and bearing stiffness effects.

3. EIGENVALUE SENSITIVITY ANALYSIS

The equation of motion of the rotating system modeled by shaft finite elements (Eq.(3)) can be rewritten in state space as follows:

$$\mathbf{A}\,\dot{\mathbf{s}} + \mathbf{B}\,\mathbf{s} = \mathbf{0} \tag{4}$$

where:

$$\mathbf{A} = \begin{bmatrix} \mathbf{0} & \mathbf{M} \\ \mathbf{M} & \mathbf{D} - \Omega\mathbf{G} \end{bmatrix} \tag{5}$$

$$\mathbf{B} = \begin{bmatrix} -\mathbf{M} & \mathbf{0} \\ \mathbf{0} & \mathbf{K} \end{bmatrix} \tag{6}$$

$$\mathbf{s} = \left\{ \begin{array}{cc} \dot{\mathbf{q}} & \mathbf{q} \end{array} \right\}^T \tag{7}$$

By assuming a harmonic solution to Eq.(4), one arrives at the eigenvalue problems of the system:

$$(\lambda_i \mathbf{A} + \mathbf{B})\, \mathbf{\Phi}_i = \mathbf{0} \tag{8}$$

$$\left(\lambda_i \mathbf{A}^T + \mathbf{B}^T\right) \mathbf{\Psi}_i = \mathbf{0} \tag{9}$$

where λ_i is the i-th eingenvalue, $\mathbf{\Phi}_i$ is the right eigenvector and, $\mathbf{\Psi}_i$ is the left eigenvector of the system. The eigenvectors, in state space formulation, satisfy the biorthogonality relations:

$$\begin{aligned} \mathbf{\Psi}_j^T \mathbf{A} \mathbf{\Phi}_i &= R_i \delta_{ij} \\ \mathbf{\Psi}_j^T \mathbf{B} \mathbf{\Phi}_i &= -\lambda_i R_i \delta_{ij} \end{aligned} \tag{10}$$

where δ_{ij} is the Kronecker delta function. The premultiplication of Eq.(8) by $\mathbf{\Psi}_i^T$ results in the scalar equation:

$$\mathbf{\Psi}_i^T \left(\lambda_i \mathbf{A} + \mathbf{B}\right) \mathbf{\Phi}_i = 0 \tag{11}$$

The differentiation of Eq.(11) with respect to a parameter p and, use of biorthogonality relationships (Eq.(10)), results in the expression for eigenvalue derivatives (Nordmann, 1982; Rajan et al. 1986):

$$\frac{\partial \lambda_i}{\partial p} = -\frac{1}{R_i} \mathbf{\Psi}_i^T \left(\lambda_i \frac{\partial \mathbf{A}}{\partial p} + \frac{\partial \mathbf{B}}{\partial p} \right) \mathbf{\Phi}_i \tag{12}$$

Equation (12) gives an expression for the derivative of the i-th eingenvalue with respect to the parameter p. As one can see, this derivative is a function of the left and right eigenvectors of the system and of the derivatives of matrices $\mathbf{A}$ and $\mathbf{B}$ with respect to p. By taking advantage of the properties of matrices $\mathbf{A}$ and $\mathbf{B}$ one can develop an efficient procedure for calculating $\partial \lambda_i / \partial p$ and tackling the inverse problem.

3.1 Element Sensitivity Matrices

To perform a shape optimization of the shaft radii as a function of the desired eigenfrequencies, one has to know the derivative of the i-th eingenvalue with respect to the shaft radius r. Hence, expanding Eq.(12), one has:

$$\frac{\partial \lambda_i}{\partial r} = -\frac{1}{R_i} \mathbf{\Psi}_i^T \left(\lambda_i \frac{\partial \mathbf{A}}{\partial r} + \frac{\partial \mathbf{B}}{\partial r} \right) \mathbf{\Phi}_i = -\frac{1}{R_i} \mathbf{\Psi}_i^T \left(\lambda_i \begin{bmatrix} \mathbf{0} & \dfrac{\partial \mathbf{M}}{\partial r} \\ \dfrac{\partial \mathbf{M}}{\partial r} & \dfrac{\partial \mathbf{D}}{\partial r} - \Omega \dfrac{\partial \mathbf{G}}{\partial r} \end{bmatrix} + \begin{bmatrix} -\dfrac{\partial \mathbf{M}}{\partial r} & \mathbf{0} \\ \mathbf{0} & \dfrac{\partial \mathbf{K}}{\partial r} \end{bmatrix} \right) \mathbf{\Phi}_i \tag{13}$$

As one can see, the calculation of $\partial \lambda_i / \partial r$ depends on the derivatives of all global matrices with respect to r. Considering that, the shaft is modeled by n_e elements and each element may have a different radius, one has to perform the derivatives with respect to each element radius r_j. Hence, the differentiation of the global matrices with respect to the radius of the j-th shaft element results in:

$$\frac{\partial \mathbf{M}}{\partial r_j} = \begin{array}{c} \begin{array}{ccc} 4j-3 & & 4j+4 \end{array} \\ \left[\begin{array}{c|c|c} \mathbf{0} & \mathbf{0} & \mathbf{0} \\ \hline \mathbf{0} & \dfrac{2}{r_j}\mathbf{M}_{ej}^T + \dfrac{4}{r_j}\mathbf{M}_{ej}^R & \mathbf{0} \\ \hline \mathbf{0} & \mathbf{0} & \mathbf{0} \end{array}\right] \end{array} \begin{array}{l} 4j-3 \\ \\ 4j+4 \end{array} \tag{14}$$

$$\frac{\partial \mathbf{G}}{\partial r_j} = \begin{array}{c} \begin{array}{ccc} 4j-3 & & 4j+4 \end{array} \\ \left[\begin{array}{c|c|c} \mathbf{0} & \mathbf{0} & \mathbf{0} \\ \hline \mathbf{0} & \dfrac{4}{r_j}\mathbf{G}_{ej} & \mathbf{0} \\ \hline \mathbf{0} & \mathbf{0} & \mathbf{0} \end{array}\right] \end{array} \begin{array}{l} 4j-3 \\ \\ 4j+4 \end{array} \tag{15}$$

$$\frac{\partial \mathbf{D}}{\partial r_j} = \mathbf{0} \tag{16}$$

$$\frac{\partial \mathbf{K}}{\partial r_j} = \begin{array}{cc} \begin{array}{ccc} \scriptstyle 4j-3 & & \scriptstyle 4j+4 \end{array} & \\ \left[\begin{array}{c|c|c} \mathbf{0} & \mathbf{0} & \mathbf{0} \\ \hline \mathbf{0} & \frac{4}{r_j}\mathbf{K}_{ej} & \mathbf{0} \\ \hline \mathbf{0} & \mathbf{0} & \mathbf{0} \end{array}\right] & \begin{array}{c} \scriptstyle 4j-3 \\ \scriptstyle 4j+4 \end{array} \end{array} \tag{17}$$

where $\mathbf{M}_{ej}^T$ and $\mathbf{M}_{ej}^R$ are the translational and rotational mass matrices of the j-th shaft element, $\mathbf{G}_{ej}$ is the gyroscopic matrix of the j-th shaft element and, $\mathbf{K}_{ej}$ is the stiffness matrix of the j-th shaft element, given by Nelson and McVaugh (1976). The damping matrix $\mathbf{D}$ does not depend on the shaft radius and depends only on the bearing damping.

As one can see, due to the characteristics of the global matrices, the derivatives with respect to the j-th shaft radius are null matrices, with non zero coefficients only in the row and columns correspondent to the j-th shaft element. Besides, these non zeros coefficients are proportional to the shaft element matrices. Hence, one can simplify Eq.(13), as follows:

$$\frac{\partial \lambda_i}{\partial r_j} = -\frac{1}{R_i}\hat{\mathbf{\Psi}}_i^T \left(\lambda_i \begin{bmatrix} \mathbf{0} & \frac{2}{r_j}\mathbf{M}_{ej}^T + \frac{4}{r_j}\mathbf{M}_{ej}^R \\ \frac{2}{r_j}\mathbf{M}_{ej}^T + \frac{4}{r_j}\mathbf{M}_{ej}^R & -\Omega\frac{4}{r_j}\mathbf{G}_{ej} \end{bmatrix} + \begin{bmatrix} -\frac{2}{r_j}\mathbf{M}_{ej}^T - \frac{4}{r_j}\mathbf{M}_{ej}^R & \mathbf{0} \\ \mathbf{0} & \frac{4}{r_j}\mathbf{K}_{ej} \end{bmatrix} \right) \hat{\mathbf{\Phi}}_i \tag{18}$$

where $\hat{\mathbf{\Psi}}_i$ contains the rows $4j-3$ to $4j+4$ and $8j-3$ to $8j+4$ of the left eigenvector $\mathbf{\Psi}_i$ and, $\hat{\mathbf{\Phi}}_i$ contains the rows $4j-3$ to $4j+4$ and $8j-3$ to $8j+4$ of the right eigenvector $\mathbf{\Phi}_i$.

Equation (18) gives an expression for the derivative of the i-th eigenvalue with respect to the j-th shaft radius. This expression depends on the right and left eigenvectors, the shaft element matrices and the shaft radius and, all this information is known after modeling the system. Hence, one arrived at a simple way of calculating $\lambda_i/\partial r_j$, which can be easily implemented computationally and has the advantage of working with reduced 16×16 matrices instead of the full $4(n_e+1)\times 4(n_e+1)$ state space matrices of Eq.(13).

4. SHAPE OPTIMIZATION ALGORITHM

In order to perform a shape optimization of the shaft as a function of the desired eigenfrequencies, one adopts the Newton-Raphson Method. An expansion in Taylor series of the i-th eigenvalue as a function of the j-th shaft radius results in:

$$\lambda_i = \lambda_i^o + \left.\frac{\partial \lambda_i}{\partial r_j}\right|^o \left(r_j - r_j^o\right) \tag{19}$$

where λ_i^o and $\partial\lambda_i/\partial r_j|^o$ are evaluated for a $r_j = r_j^o$.

Thus, the inverse problem is given by:

$$r_j = r_j^o + \left(\left.\frac{\partial \lambda_i}{\partial r_j}\right|^o \right)^{-1} \left(\lambda_i - \lambda_i^o\right) \tag{20}$$

The Newton-Raphson Method adopts Eq.(20) as an updating law in the recursive algorithm. Hence, for the n-th iteration of the algorithm, one has:

$$r_j^{n+1} = r_j^n + \left(\left.\frac{\partial \lambda_i}{\partial r_j}\right|^n \right)^{-1} \left(\lambda_i^R - \lambda_i^n\right) \tag{21}$$

where λ_i^R is the desired eigenvalue (reference).

If the system has n_e shaft elements and one considers m eigenvalues, the iteration equation (21) can be rewritten as follows:

$$\mathbf{r}_{n_e\times 1}^{n+1} = \mathbf{r}_{n_e\times 1}^{n} + \left(\mathbf{J}^n\right)_{n_e\times m}^{-1} \left(\mathbf{\Lambda}^R - \mathbf{\Lambda}^n\right)_{m\times 1} \tag{22}$$

where $\mathbf{r}$ contains the n_e shaft radii r_j, $\mathbf{\Lambda}$ contains the m eigenvalues, $\mathbf{\Lambda}^R$ contains the m desired eigenvalues and, $\mathbf{J}$ is the Jacobian matrix, given by:

$$\mathbf{J} = \begin{bmatrix} \frac{\partial\lambda_1}{\partial r_1} & \frac{\partial\lambda_1}{\partial r_2} & \cdots & \frac{\partial\lambda_1}{\partial r_{n_e}} \\ \frac{\partial\lambda_2}{\partial r_1} & \frac{\partial\lambda_2}{\partial r_2} & \cdots & \frac{\partial\lambda_2}{\partial r_{n_e}} \\ \vdots & \vdots & & \vdots \\ \frac{\partial\lambda_m}{\partial r_1} & \frac{\partial\lambda_m}{\partial r_2} & \cdots & \frac{\partial\lambda_m}{\partial r_{n_e}} \end{bmatrix}_{m\times n_e} \tag{23}$$

Equation (22) can be used to calculate the necessary radii of each shaft element in the rotating system for achieving the desired $\mathbf{\Lambda}^R$ eigenvalues. The iteration procedure can be stopped when the norm $\left|\mathbf{\Lambda}^R - \mathbf{\Lambda}^n\right|$ lies within an adopted tolerance. If $n_e \neq m$, then a pseudo-inverse operation must be adopted in the procedure for finding $(\mathbf{J}^n)^{-1}$.

Experience shows that the algorithm has good convergence when $n_e \geq m$. In the case that $n_e < m$, i.e. the number of desired eigenvalues is greater than the number of shaft elements in the model, one suggests to increase the number of elements that represent the model. This procedure will not jeopardize the results and will guarantee the algorithm convergence.

4.1 Numerical Results

The rotating system in study is composed of three disks, supported by two self aligning ball bearings, and whose dimensions are shown in Fig.1. Its operational range is between 60 and 70 Hz (rotating frequency).

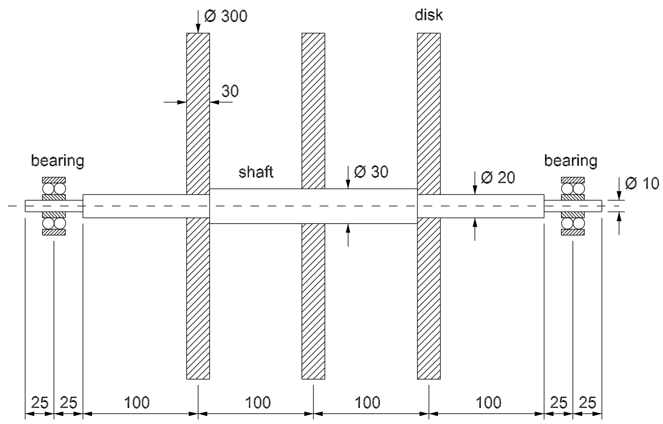

Figure 1. Rotating system in study (dimensions in mm).

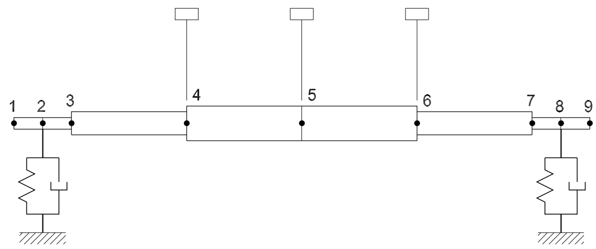

Figure 2. Finite element model of the rotating system.

This rotating system can be modeled by finite elements as shown in Fig.2. The resultant model has 8 shaft elements, 9 nodes and, the inertia and gyroscopic effects of the disks are located at nodes 4, 5 and 6. The bearing damping and stiffness are located at nodes 2 and 8. Considering that one has ball bearings, the adopted stiffness is 10^8 N/m and the adopted damping is 10 $N/m/s$, in each orthogonal directions (translations). No cross-coupling coefficients were adopted for damping and stiffness.

The Campbell diagram of the rotating system in study is presented in Fig.3. As one can see, the system crosses its first two critical speeds, related to the first bending modes of the shaft, at 35.9 Hz and 37.5 Hz. The third critical speed, related to the second bending mode of the shaft, lies within the operational range of the system, at 66.7 Hz. This is an unacceptable condition and it is necessary to change the system to avoid such resonances at the operational range.

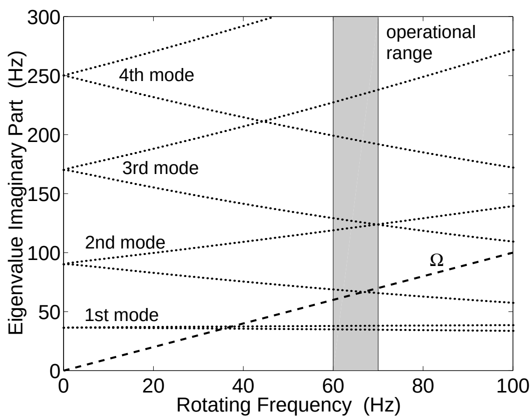

Figure 3. Campbell diagram of the rotating system in study (pristine condition).

The proposed procedure is applied to find the necessary shaft radii that shift the second critical speed beyond the operational range of the system. In addition, it is interesting to keep the first two critical speeds unchanged, because they are far from the operational range. This is done by keeping the natural frequency of the first mode unchanged and changing the natural frequency of the second mode, at null rotating frequency ($\Omega = 0$). The natural frequency associated to the first bending mode of the shaft has a value of 36.4 Hz at $\Omega = 0$ and, the natural frequency associated to the second bending mode of the shaft has a value of 90.2 Hz at $\Omega = 0$ (Fig.3). Hence, by choosing the second natural frequency as 120 Hz at $\Omega = 0$, the reference vector with desired eigenvalues has the form:

$$\mathrm{Im}(\mathbf{\Lambda}^R) = \left\{ \begin{array}{c} 228.71 \\ 228.71 \\ 753.98 \\ 753.98 \end{array} \right\} rad/s \equiv \left\{ \begin{array}{c} 36.4 \\ 36.4 \\ 120.0 \\ 120.0 \end{array} \right\} Hz \tag{24}$$

where $\mathbf{\Lambda}^R$ only contains the positive imaginary part of the desired eigenvalues. The negative imaginary part of the desired eigenvalues has similar values, with opposite signal, and will present same sensitivity. Hence, they are not considered for simplicity. The reference vector is composed of 4 eigenvalues ($m = 4$), whereas there are 8 shaft elements ($n_e = 8$). Thus, this is a condition where $n_e > m$ and convergence is guaranteed. The procedure resulted in the shaft radii listed in Tab.1, considering two modes.

The Campbell diagram of the rotating system with the optimized shaft considering two modes is presented in Fig.4(a). As one can see, the system crosses its first two critical speeds at 33.8 Hz and 40.5 Hz, thus not representing a major change compared to the pristine condition. The third critical speed, related to the second bending mode of the shaft, now lies beyond the operational range of the system, at 87.6 Hz. Hence, the objective of keeping the first two critical speeds and shifting the third critical speed beyond the operational range has been accomplished. The frequency response function of the shaft at null rotating frequency (Fig.4(b)) shows that the first natural frequency remained unchanged at 36.4 Hz, whereas the second natural frequency was successfully moved to 120 Hz.

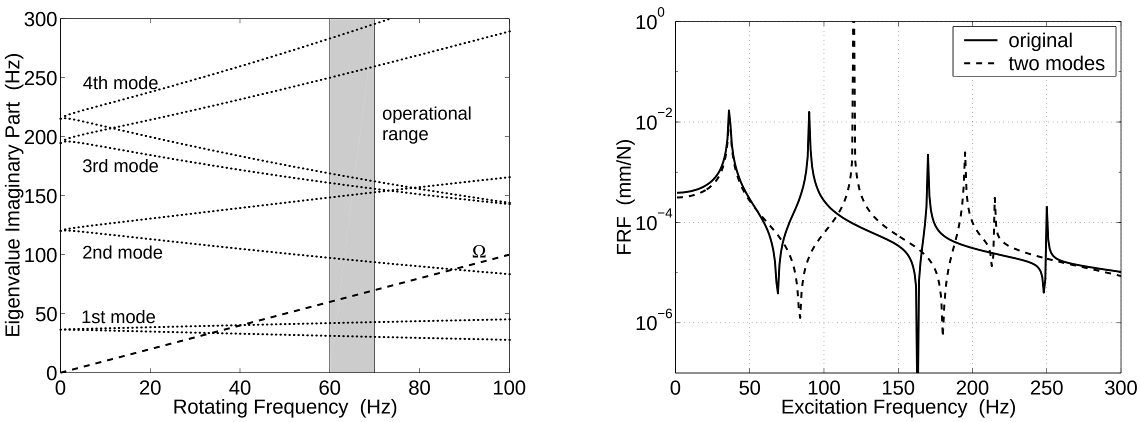

(a) Campbell diagram

(b) Frequency response function at $\Omega = 0$

Figure 4. Dynamic behavior of the rotating system with optimized shaft considering 2 modes.

It is interesting to note that, the natural frequencies not considered in the optimization procedure (3rd and 4th modes) also presented different values from those of the pristine condition (Fig.4(b)). This is a consequence of only choosing the eigenvalues related to the first two modes of the system. The optimization procedure looked for a solution that fulfilled the requirements stated by Eq.(24) and, the solution was found disregarding the effects on the remaining natural frequencies.

Alternatively, the procedure also works considering more frequencies. For example, one can keep the natural frequency of the first, third and fourth modes unchanged and change the natural frequency of the second mode, at null rotating frequency ($\Omega = 0$). The natural frequencies associated to the third and fourth bending modes of the shaft have values of 170.1 and 250.1 Hz, respectively, at $\Omega = 0$ (Fig.3). Hence, by choosing the second natural frequency as 120 Hz, the reference vector with desired eigenvalues has the form:

$$\mathrm{Im}(\mathbf{\Lambda}^R) = \left\{ \begin{array}{r} 228.71 \\ -228.71 \\ 753.98 \\ -753.98 \\ 1068.77 \\ -1068.77 \\ 1571.42 \\ -1541.42 \end{array} \right\} rad/s \equiv \left\{ \begin{array}{c} 36.4 \\ 36.4 \\ 120.0 \\ 120.0 \\ 170.1 \\ 170.1 \\ 250.1 \\ 250.1 \end{array} \right\} Hz \tag{25}$$

Again, $\mathbf{\Lambda}^R$ only contains the positive imaginary part of the desired eigenvalues and the negative imaginary part was not considered for simplicity. The reference vector is composed of 8 eigenvalues ($m = 8$), thus this is a condition where $n_e = m$ and convergence is guaranteed. The procedure resulted in the shaft radii listed in Tab.1, considering four modes.

The Campbell diagram of the rotating system with the optimized shaft considering four modes is presented in Fig.5(a). As one can see, the system crosses its first two critical speeds at 33.8 Hz and 39.7 Hz, again not representing a major change compared to the pristine condition. The third critical speed, related to the second bending mode of the shaft, also lies beyond the operational range of the system, at 87.3 Hz. Hence, the objective of keeping the first two critical speeds and shifting the third critical speed beyond the operational range has been accomplished. The frequency response function of the shaft at null rotating frequency (Fig.5(b)) shows that the first, third and fourth natural frequencies were minimally changed to 36.2 Hz, 169.7 Hz and 249.4 Hz, whereas the second natural frequency was successfully moved to 120 Hz. This slight change in the natural frequencies are caused by rounding errors in the values of shaft radii presented in Tab.1 (the solution has more than one decimal value).

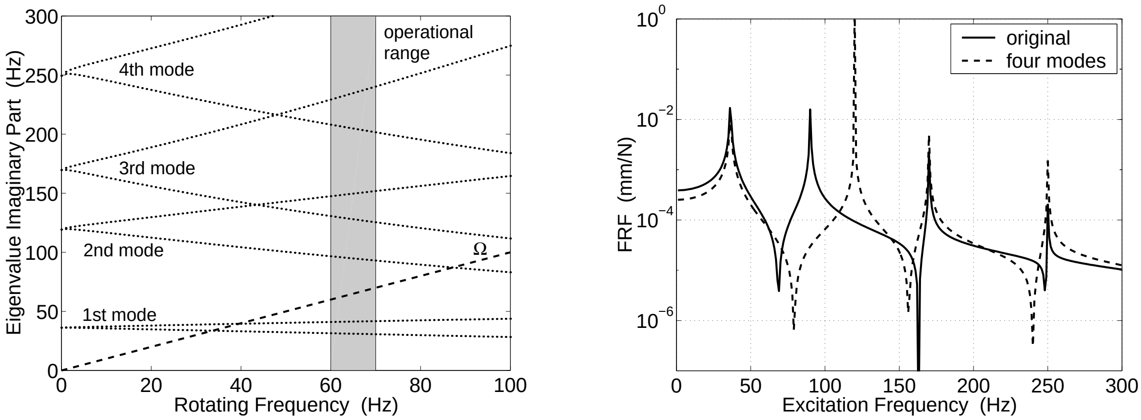

(a) Campbell diagram

(b) Frequency response function at $\Omega = 0$

Figure 5. Dynamic behavior of the rotating system with optimized shaft considering 2 modes.

Table 1. Shaft radii obtained by the shape optimization procedure (dimensions in mm).

condition	r_1	r_2	r_3	r_4	r_5	r_6	r_7	r_8	shape
pristine	5.0	5.0	10.0	15.0	15.0	10.0	5.0	5.0	
2 modes	5.9	5.9	12.8	12.8	12.8	12.8	5.9	5.9	
4 modes	6.3	6.3	14.0	14.5	12.2	10.6	6.2	6.2	

As one can see, the procedure managed to find a shape solution to the shaft that presents the desired natural frequencies (Tab.1). Again, the optimization procedure looked for a solution that fulfilled the requirements stated by Eq.(25), and the solution was found disregarding the effects on the remaining natural frequencies. Nothing can be said about the other natural frequencies not considered in the analysis (fifth, sixth, etc).

5. CONCLUSIONS

In this work, one presents a practical, low time consuming procedure for finding the shaft geometry (shaft radii) of rotating machines, whose dynamic characteristics results in desired eigenfrequencies and critical speeds.

The numerical examples show that it is possible to find design solutions for the shaft, keeping certain natural frequencies at null rotating frequency unchanged whereas others are moved to desired values. Considering that the procedure performs a modal reduction during the evaluation of the sensitivity parameters, nothing can be said about the unconsidered natural frequencies in the analysis. These frequencies will probably change by the adoption of the found design solution.

The procedure has good convergence when the number of shaft elements are greater or equal the number of considered eigenvalues ($n_e \geq m$). A satisfactory solution for the case that $n_e < m$ is refining the model by adding more shaft elements. Refining the model will not jeopardize the results (it actually improves precision) and will guarantee the algorithm convergence.

By adopting the proposed optimization algorithm, one can obtain reasonable design solutions for the shaft. This procedure can help engineers to find the best solution for their rotating machine in early stages of design. The procedure can also be used for model updating, setting the experimentally measured frequencies as desired frequencies, and obtaining the updated shaft shape (radii) to be used in the model.

6. REFERENCES

Fang, Z., Wang, M., 2003, "A New Method Seeking Optimal Parameters and Locations for Bearings of Rotating Machinery Systems", Proceedings of 19th Biennial ASME Conference on Mechanical Vibration and Noise, Vol.5, Chicago, USA, pp.2045-2049.

Huang, S.C., Lin, C.A., 2002, "Sensitivity Analysis and Optimization of Undamped Rotor Critical Speeds to Support Stiffness", Journal of Vibration and Acoustics, Vol.124, No.2., pp.296-301.

Lund, J.W., 1980, "Sensitivity of the Critical Speeds of a Rotor to Changes in the Design", Journal of Mechanical Design, Vol.102, No.1, pp.115-121.

Nelson, H.D., McVaugh, J.M, 1976, "The Dynamics of Rotor-Bearing Systems Using Finite Element", Journal of Engineering for Industry, Vol.98, No.2, pp.593-600.

Nordmann, R., 1982, "Modal Parameter Identification and Sensitivity Analysis in Rotating Machinery", Proceedings of the International Conference Rotor Dynamic Problems in Power Plant, Rome, Italy, pp.95-102.

Rajan, M., Nelson, H.D., Chen, W.J., 1986, "Parameter Sensitivity in the Dynamics of Rotor-Bearing Systems", Journal of Vibration, Acoustics, Stress, and Reliability in Design, Vol.108, No.2, pp.197-206.

Silveira, Z.C., Lucchesi, K.C., 2004, "Statistical Analysis and Optimization of Design Parameters in Components of Rotating Machinery", Proceedings of 8th International Conference on Vibrations in Rotating Machinery, Swansea, UK, pp.615-626.

Yoo, H.H., Cho, J.E., Chung, J., 2006, "Modal Analysis and Shape Optimization of Rotating Cantilever Beams", Journal of Sound and Vibration, Vol.290, No.1-2, pp.223-241.

7. Responsibility notice

The author is the only responsible for the printed material included in this paper.